Inorg. Chem. **1993**, *32*, 2360–2365

Rhodium(I) and Rhodium(III) Phosphine Complexes with Nonbridging Benzenethiolato Ligands: Preparation, Structures, and Chemical Properties

Kohtaro Osakada,* Kouji Hataya, and Takakazu Yamamoto*

Research Laboratory of Resources Utilization, Tokyo Institute of Technology, 4259 Nagatsuta, Midori-ku, Yokohama 227, Japan

Received September 4, 1992

Reactions of NaSPh with $[Rh(PMe_3)_4]Cl$ and with $RhCl(PMe_3)_3$ give $Rh(SPh)(PMe_3)_3$ (**1**), whose X-ray crystallography shows a square-planar coordination. Temperature-dependent NMR (^1H and $^{31}P\{^1H\}$) spectra of **1** show fluxionality of the molecule due to intramolecular exchange of the ligands in the solution. Complex **1** reacts smoothly with air to give the dioxygen-coordinated complex $Rh(SPh)(O_2)(PMe_3)_3$ (**2**). X-ray crystallography shows a distorted trigonal bipyramidal coordination around the metal center having a dioxygen ligand with the O–O bond distance of 1.456(6) Å. Addition of air to the reaction mixture of $[Rh(PMe_3)_4]Cl$ with $NaSC_6H_4$-*p*-OMe gives the analogous dioxygen-coordinated complex $Rh(SC_6H_4$-*p*-$OMe)(O_2)(PMe_3)_3$ (**3**). Reaction of complex **1** with HSPh in hexane causes oxidative addition of the S–H bond to the metal center to give the Rh(III) complex *cis,mer*-$RhH(SPh)_2(PMe_3)_3$ (**4a**) as the initial product. Further stirring of the reaction mixture at room temperature causes isomerization of **4a** into *trans,mer*-$RhH(SPh)_2(PMe_3)_3$ (**4b**). NMR (^1H and ^{31}P) spectra of the complexes **4a** and **4b** as well as X-ray crystallography of **4b** indicate their respective structures unambiguously. Reaction of DSPh (65% D) with **4a** gives *trans,mer*-$RhD(SPh)_2(PMe_3)_3$ (**4b**-d_1) in 55% isotopic purity, while similar reaction with **4b** causes deuteration in 18%. Reaction of phenyl acetylene with complex **1** gives *mer*-$RhH(C{\equiv}CPh)(SPh)(PMe_3)_3$ (**5**) with the acetylide and the thiolato ligands at mutually trans positions.

Introduction

Properties of transition metal thiolato complexes[1-9] have attracted increasing attention in view of the important roles which these compounds are believed to play as intermediates in various reactions such as desulfurization of organosulfur compounds,[10-15] metal-catalyzed synthetic organic reactions involving C–S bond cleavage and formation,[16-22] and preparation of transition metal sulfides through degradation of the thiolato ligands.[23-26] Preparation of simple rhodium(I) thiolato complexes having tertiary phosphine as the auxiliary ligands, $Rh(SR)(PR'_3)_n (n = 3$ or 4), and investigation of their chemical properties seems to be intriguing because some of the above reactions involve rhodium thiolato phosphine complexes as the intermediates. Actually Rh(III)–triphos complexes having Rh–S bonds were reported to show remarkable reactivity toward organic and inorganic reagents.[27] On the other hand, there have been few reports concerning mononuclear Rh(I) thiolato complexes whose metal center and thiolato ligands would show higher reactivity toward electrophilic compounds than those of already known dinuclear Rh(I)–diene or Rh(I)–PPh_3 complexes with bridging thiolato ligands.[28-31] Reaction of $RhH(PPh_3)_4$ with thiophenol gave $[Rh(\mu\text{-}SPh)(PPh_3)_2]_2$ through initial formation of Rh(SPh)(P-

---

(1) DuBois, M. R. *Chem. Rev.* **1989**, *89*, 1 and references therein.
(2) Tatsumi, K.; Sekiguchi, Y.; Nakamura, A.; Cramer, R. E.; Rupp, J. J. *J. Am. Chem. Soc.* **1986**, *108*, 1358.
(3) (a) Osakada, K.; Maeda, M.; Nakamura, Y.; Yamamoto, T.; Yamamoto, A. *J. Chem. Soc., Chem. Commun.* **1986**, 442. (b) Osakada, K.; Chiba, T.; Nakamura, Y.; Yamamoto, T.; Yamamoto, A. *Ibid.* **1986**, 1589. (c) Kim, Y.-J.; Osakada, K.; Sugita, K.; Yamamoto, T.; Yamamoto, A. *Organometallics* **1988**, *7*, 2182. (d) Osakada, K.; Chiba, T.; Yamamoto, T.; Yamamoto, A. *Ibid.* **1989**, *8*, 2602. (e) Osakada, K.; Ozawa, Y.; Yamamoto, A. *J. Chem. Soc., Dalton Trans.* **1991**, 759.
(4) Bulman Page, P. C.; Klair, S. S.; Brown, M. P.; Harding, M. M.; Smith, C. S.; Maginn, S. J.; Mulley, S. *Tetrahedron Lett.* **1988**, *29*, 4477.
(5) (a) Amarasekera, J.; Rauchfuss, T. B.; Wilson, S. R. *J. Chem. Soc., Chem. Commun.* **1989**, 14. (b) Amarasekera, J.; Rauchfuss, T. B. *Inorg. Chem.* **1989**, *28*, 3875.
(6) (a) Dev, S.; Imagawa, K.; Mizobe, Y.; Cheng, G.; Wakatsuki, Y.; Yamazaki, H.; Hidai, M. *Organometallics* **1989**, *8*, 1232. (b) Dev, S.; Mizobe, Y.; Hidai, M. *Inorg. Chem.* **1990**, *29*, 4797. (c) Matsuzaka, H.; Mizobe, Y.; Nishio, M.; Hidai, M. *J. Chem. Soc., Chem. Commun.* **1991**, 1011.
(7) Liaw, W.-F.; Kim, C.; Darensbourg, M. Y.; Rheingold, A. L. *J. Am. Chem. Soc.* **1989**, *111*, 3591.
(8) (a) Klein, D. P.; Kloster, G. M.; Bergman, R. G. *J. Am. Chem. Soc.* **1990**, *112*, 2022. (b) Carney, M. J.; Walsh, P. J.; Bergman, R. G. *Ibid.* **1990**, *112*, 6426. (c) Michelman, R. I.; Anderson, R. A.; Bergman, R. G. *Ibid.* **1991**, *113*, 5100.
(9) (a) Jones, W. D.; Dong, L. *J. Am. Chem. Soc.* **1991**, *113*, 559. (b) Dong, L.; Duckett, S. B.; Ohman, K. F.; Jones, W. D. *Ibid.* **1992**, *114*, 151.
(10) Kwart, H.; Schuit, G. C. A.; Gates, B. C. *J. Catal.* **1980**, *61*, 128.
(11) Zaera, F.; Kollin, E. B.; Gland, J. L. *Surf. Sci.* **1987**, *184*, 75.
(12) Eisch, J. J.; Hallenbeck, L. E.; Han, K. I. *J. Org. Chem.* **1983**, *48*, 2963.
(13) (a) Alper, H.; Blais, C. *J. Chem. Soc., Chem. Commun.* **1980**, 169. (b) Antebi, S.; Alper, H. *Organometallics* **1986**, *5*, 596.
(14) (a) Angelici, R. J. *Acc. Chem. Res.* **1988**, *21*, 387. (b) *Coord. Chem. Rev.* **1990**, *105*, 61. (c) Chen, J.; Angelici, R. J. *Organometallics* **1992**, *11*, 992.
(15) (a) Rauchfuss, T. B. *Prog. Inorg. Chem.* **1991**, *39*, 259. (b) Luo, S.; Skaugset, A. E.; Rauchfuss, T. B.; Wilson, S. R. *J. Am. Chem. Soc.* **1992**, *114*, 1732.
(16) (a) Okamura, H.; Miura, M.; Takei, H. *Tetrahedron Lett.* **1979**, 43. (b) Okamura, H.; Takei, H. *Ibid.* **1979**, 3425.
(17) Murahashi, S.; Yamamura, M.; Yanagisawa, K.; Mita, N.; Kondo, K. *J. Org. Chem.* **1979**, *44*, 2408.
(18) (a) Kosugi, M.; Shimizu, T.; Migita, T. *Chem. Lett.* **1978**, 13. (b) Migita, T.; Shimizu, T.; Asami, Y.; Shiobara, J.; Kato, Y.; Kosugi, M. *Bull. Chem. Soc. Jpn.* **1980**, *53*, 1385.
(19) Hutchins, R. O.; Learn, K. *J. Org. Chem.* **1982**, *48*, 4380.
(20) (a) Wenkert, E.; Ferreira, T. W.; Michelotti, E. L. *J. Chem. Soc., Chem. Commun.* **1979**, 637. (b) Wenkert, E.; Leftin, M. H.; Michelotti, E. L. *Ibid.* **1984**, 617. (c) Wenkert, E.; Hanna, J. M., Jr.; Leftin, M. H.; Michelotti, E. L.; Potts, K. T.; Usifer, D. *J. Org. Chem.* **1985**, *50*, 1125.
(21) Tiecco, M.; Testaferri, L.; Tingoli, M.; Chianelli, P.; Wenkert, E. *Tetrahedron Lett.* **1982**, *23*, 4629.
(22) Osakada, K.; Yamamoto, T.; Yamamoto, A. *Tetrahedron Lett.* **1987**, *27*, 6321.
(23) (a) Osakada, K.; Yamamoto, T. *J. Chem. Soc., Chem. Commun.* **1987**, 1117. (b) *Idem. Inorg. Chem.* **1991**, *30*, 2328.
(24) Bochmann, M.; Hawkins, I.; Wilson, L. M. *J. Chem. Soc., Chem. Commun.* **1988**, 344.
(25) Brennan, J. G.; Siegrist, T.; Carroll, R. J.; Stuczynski, S. M.; Brus, L. E.; Steigerwald, M. L. *J. Am. Chem. Soc.* **1989**, *111*, 4141.
(26) (a) Nomura, R.; Konishi, K.; Futenma, S.; Matsuda, H. *Appl. Organomet. Chem.* **1990**, *4*, 607. (b) Nomura, R.; Fujii, S.; Kanaya, K.; Matsuda, H. *Polyhedron* **1990**, *9*, 361. (c) Nomura, R.; Konishi, K.; Matsuda, H. *Thin Solid Films* **1991**, *198*, 339.
(27) (a) Bianchini, C.; Mealli, C.; Meli, A.; Sabat, M. *Inorg. Chem.* **1986**, *25*, 4617. (b) Bianchini, C.; Meli, A.; Dapporto, P.; Tofanari, A.; Zanello, P. *Ibid.* **1987**, *26*, 3677. (c) Bianchini, C.; Meli, A. *Ibid.* **1987**, *26*, 4268.
(28) Cruz-Garritz, D.; Garcia-Alejandre, J.; Torrens, H.; Alvarez, C.; Toscano, R. A.; Poilblanc, R.; Thorez, A. *Transition Met. Chem.* **1991**, *16*, 130.

0020-1669/93/1332-2360$04.00/0

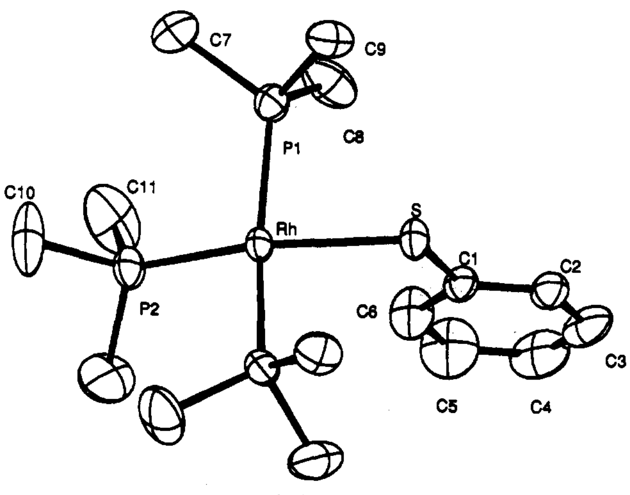

Figure 1. Molecular structure of Rh(SPh)$(PMe_3)_3$ (**1**) showing ellipsoidal plotting at 50% level. The molecule has a crystallographic mirror plane that includes the Rh, S, C1–C6, and C10 atoms.

Table I. Selected Bond Distances and Angles of **1**

Distances (Å)			
Rh–S	2.428(2)	Rh–P1	2.292(2)
Rh–P2	2.229(3)	S–C1	1.748(9)
Angles (deg)			
S–Rh–P1	85.72(5)	S–Rh–P2	162.99(9)
P1–Rh–P1′	162.3(1)	P1–Rh–P2	96.36(5)
Rh–S–C1	105.0(3)		

$Ph_3)_3$, which could not be isolated.[29,30] This is probably due to facile dissociation of the PPh_3 ligand of Rh(SPh)$(PPh_3)_3$ to give coordinatively unsaturated intermediates such as [Rh(SPh)$(PPh_3)_2$].

We have investigated the preparation of rhodium complexes with nonbridging thiolato ligands by reaction of $[Rh(PMe_3)_4]Cl$, having nonlabile PMe_3 ligands, with NaSPh. The obtained complex, Rh(SPh)$(PMe_3)_3$, reacted with various compounds such as O_2, HSPh, and HC≡CPh to give the corresponding dioxygen-coordinated Rh complex and Rh(III) hydride complexes with thiolato and acetylide ligands, respectively. Here we report the preparation, structure, and chemical properties of these rhodium thiolato complexes.

Results and Discussion

Preparation and Characterization of Rh(SPh)$(PMe_3)_3$ (1). The ionic complex $[Rh(PMe_3)_4]Cl$ reacts with NaSPh in hexane to give Rh(SPh)$(PMe_3)_3$ (**1**) as orange red microcrystals. Reaction of $RhCl(PMe_3)_3$ with NaSPh also gives complex **1**. Complex **1** is stable in benzene and toluene solution under argon and does not dimerize to give a dinuclear complex with bridging thiolato ligands. Figure 1 shows the molecular structure of **1** determined by X-ray crystallography. The molecule has a somewhat distorted square-planar coordination around the metal center. Table I summarizes selected bond distances and angles. The Rh–P1 bond is larger than the Rh1–P2 bond, indicating larger trans influence of the PMe_3 ligands than that of the SPh ligand. The Rh–S–C1 bond angle is 105°, which is more acute than in most transition metal benzenethiolato complexes.[31]

$$[Rh(PMe_3)_4]\,Cl \;+\; NaSPh \xrightarrow{-\,NaCl} \underset{\mathbf{1}}{Rh(SPh)(PMe_3)_3} \;+\; PMe_3$$

The ${}^1H$ NMR spectrum of **1** in C_6D_6 (100 MHz at 25 °C) shows a singlet at 1.15 ppm due to the PMe_3 hydrogens and signals at 6.9–8.3 ppm due to the SPh hydrogens. Figure 2 shows the ${}^{31}P\{{}^1H\}$ and ${}^1H$ NMR spectra (200 and 500 MHz, respectively) of the complex at 25, –60, and –80 °C in toluene-d_8. The ${}^1H$ and ${}^{31}P\{{}^1H\}$ NMR spectra at –80 °C agree with the square-planar coordination of the molecule. On raising of the temperature, the peaks of PMe_3 hydrogens in the ${}^1H$ NMR spectra undergo coalescence to give a single peak at 25 °C, while similar coalescence of the signals spectra is also observed in the ${}^{31}P\{{}^1H\}$ NMR. The fluxional behavior is believed due to the intramolecular ligand exchange since the peak width of the ${}^{31}P\{{}^1H\}$ NMR spectra does not change upon addition of PMe_3 or by changing the complex concentration. This dynamic behavior may involve mutual exchange of the coordination sites of the ligands through a tetrahedral transition state.

The ${}^{31}P\{{}^1H\}$ NMR spectrum at 25 °C shows quite a small doublet signal at ca. –7 ppm (with the asterisk in Figure 2). This can be tentatively assigned to a minor Rh-containing species such as $[Rh(PMe_3)_3]^+SPh^-$, which is in equilibrium with **1** in the solution although it is not characterized due to the low concentration (<3%).

Recently Anderson and his co-workers have reported the preparation and NMR spectra of the methylrhodium complex $RhMe(PMe_3)_3$ as well as of $RhMe(PMe_3)_4$.[33] The NMR spectra of the complexes near room temperature also showed that all the phosphine ligands were magnetically equivalent although at lower temperature the spectra showed rigid square-planar and trigonal-bypyramidal structures, respectively. Since $RhMe(PMe_3)_3$ does not undergo dissociation of the methyl ligand, it seems to undergo intramolecular ligand exchange that is responsible for the fluxional behavior.

Reaction of Complex 1 with O_2. Complex **1** readily reacts with air both in the solid state and in solution to give the dioxygen-coordinated complex Rh(SPh)$(O_2)(PMe_3)_3$ (**2**) as a yellow solid.

$$\underset{\mathbf{1}}{Rh(SPh)(PMe_3)_3} \;+\; O_2 \longrightarrow \underset{\mathbf{2}}{Rh(SPh)(O_2)(PMe_3)_3}$$

The compound is obtained also by direct reaction of oxygen with the reaction mixture of $[Rh(PMe_3)_4]Cl$ with NaSPh. A similar complex with a dioxygen ligand, Rh$(SC_6H_4$-*p*-OMe$)(O_2)(PMe_3)_3$ (**3**), is prepared by reaction of air with the reaction mixture of $[Rh(PMe_3)_4]Cl$ with $NaSC_6H_4$-*p*-OMe. The reaction is considered to proceed through initial formation of Rh(I) thiolato complex such as Rh$(SC_6H_4$-*p*-OMe$)(PMe_3)_n$ (*n* = 3 or 4) followed by its reaction with oxygen. However, extremely high sensitivity of the intermediate thiolato complex prevents its isolation.

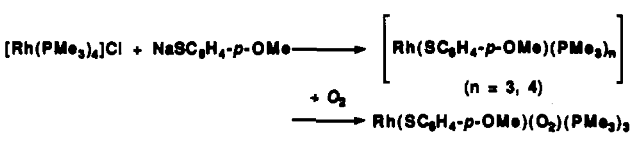

$$[Rh(PMe_3)_4]Cl + NaSC_6H_4\text{-}p\text{-}OMe \longrightarrow \left[\underset{(n = 3,\ 4)}{Rh(SC_6H_4\text{-}p\text{-}OMe)(PMe_3)_n}\right] \xrightarrow{+\,O_2} \underset{\mathbf{3}}{Rh(SC_6H_4\text{-}p\text{-}OMe)(O_2)(PMe_3)_3}$$

Previously $RhCl(PPh_3)_3$ was reported to react with oxygen to give a similar dioxygen-coordinated rhodium complex $RhCl(O_2)(PPh_3)_3$ or $[RhCl(O_2)(PPh_3)_2]_2$ depending on the reaction conditions.[34] These Rh–PPh_3 complexes with η^2-dioxygen ligands were reported to promote oxidative ring expansion of bicyclic compounds[35] and were postulated as the active species in oxidation

---

[29] Osakada, K.; Matsumoto, K.; Yamamoto, T.; Yamamoto, A. *Organometallics* **1985**, *4*, 857.

[30] Carlton, L.; Bulbulia, Z. *J. Organomet. Chem.* **1990**, *389*, 139.

[31] (a) Kalck, P.; Poilblanc, R. *Inorg. Chem.* **1975**, *14*, 2779. (b) Bonnet, J. J.; Kalck, P.; Poilblanc, R. *Ibid.* **1977**, *16*, 1514.

[32] Ashby, M. T. *Comments Inorg. Chem.* **1990**, *10*, 297.

[33] Price, R. T.; Anderson, R. A.; Muetterties, E. L. *J. Organomet. Chem.* **1989**, *376*, 407.

[34] (a) Bennett, M. J.; Donaldson, P. B. *J. Am. Chem. Soc.* **1971**, *93*, 3307. (b) *Inorg. Chem.* **1977**, *16*, 1581 and 1585.

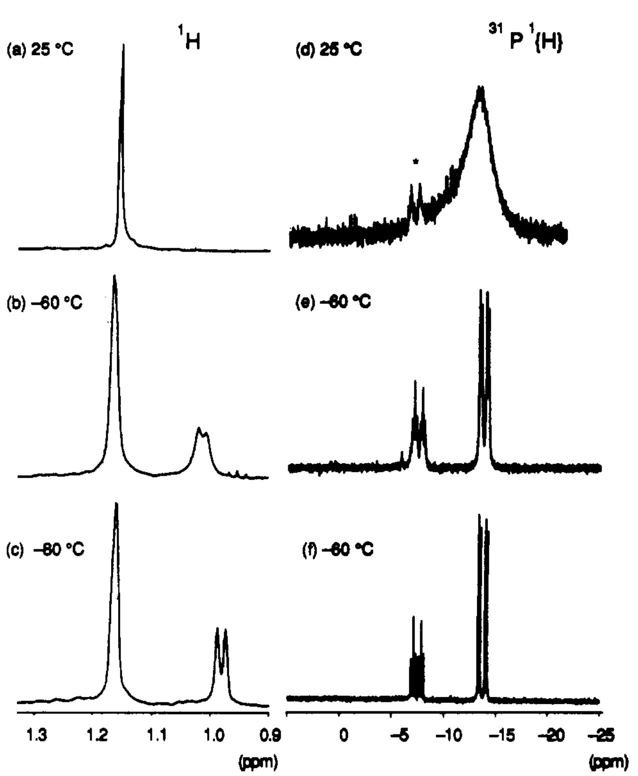

Figure 2. ^{1}H and ^{31}P{^{1}H} NMR spectra of 1 in toluene-d_8 at 500 MHz and at 200 MHz, respectively. (a) P(CH$_3$)$_3$ hydrogen region of ^{1}H NMR spectra at 25 °C, (b) at -60 °C, and (c) at -80 °C. (d) ^{31}P{^{1}H} NMR spectra at 25 °C, (e) at -60 °C, and (f) at -80 °C.

Table II. Selected Bond Distances and Angles of 2

	Distances (Å)		
Rh-S	2.393(2)	Rh-P1	2.333(2)
Rh-P2	2.333(2)	Rh-P3	2.295(1)
Rh-O1	2.041(3)	Rh-O2	2.015(4)
S-C1	1.765(6)	O1-O2	1.456(6)
	Angles (deg)		
S-Rh-P1	97.08(6)	S-Rh-P2	89.63(6)
S-Rh-P3	86.49(6)	P1-Rh-P2	164.49(5)
P1-Rh-P3	97.10(6)	P2-Rh-P3	97.25(6)
O1-Rh-S	117.2(1)	O1-Rh-P1	86.0(2)
O1-Rh-P2	78.5(2)	O1-Rh-P3	155.7(2)
O2-Rh-S	159.1(1)	O2-Rh-P1	80.7(1)
O2-Rh-P2	88.0(1)	O2-Rh-P3	114.5(1)
O1-Rh-O2	42.1(1)	Rh-O1-O2	68.0(2)
Rh-O2-O1	69.9(2)	Rh-S-C1	111.8(2)

of olefins promoted by Rh complexes.[36] In the present reactions using PMe$_3$ ligands we have obtained the complexes with three PMe$_3$ ligands exclusively probably due to less labile nature of PMe$_3$ than PPh$_3$.

Figure 3 shows the molecular structure of 2 determined by X-ray crystallography. The molecule has a trigonal bipyramidal coordination around the rhodium center. Table II summarizes selected bond distances and angles of the complex. The dioxygen molecule is coordinated in a side-on fashion. The O–O bond distance is 1.456(6) Å, which is considerably longer than that of free dioxygen (1.21 Å) and comparable to that of H_2O_2 (1.49 Å). The elongation of the O–O bond distance of the dioxygen molecule is observed also in the already reported Rh dioxygen complexes such as RhCl(O$_2$)(PPh$_3$)$_3$ (1.413(9) Å) and [RhCl(O$_2$)(PPh$_3$)$_2$]$_2$ (1.44(1) Å).

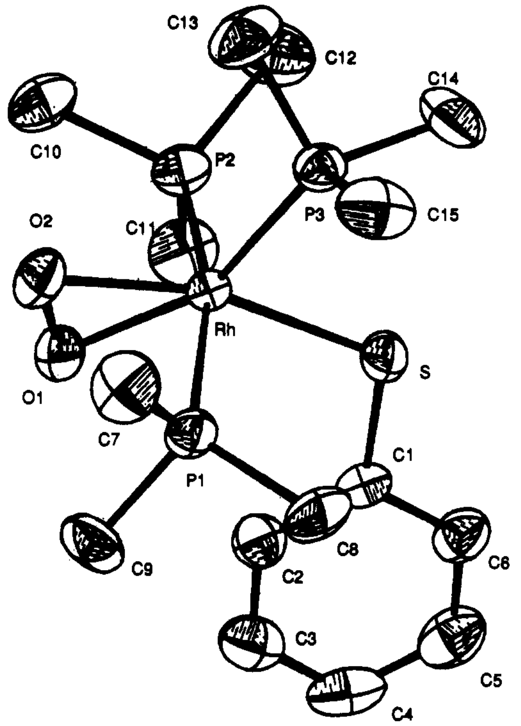

Figure 3. Molecular structure of Rh(SPh)(O$_2$)(PMe$_3$)$_3$ (2) showing ellipsoidal plotting at 50% level.

NMR (^{1}H and ^{31}P{^{1}H}) spectra of complexes 2 and 3 agree with the proposed structures. ^{1}H NMR spectra of the complexes show PMe$_3$ hydrogen signals as a doublet and a triplet due to virtual coupling[37] in a 1:2 peak area ratio. They are assigned as a peak due to the PMe$_3$ ligand at an equatorial position and that due to the two PMe$_3$ ligands on the apical positions. ^{31}P{^{1}H} NMR spectra agree well with the simulated spectra by assuming an A$_2$BX pattern. Figure 4 shows the observed and simulated ^{31}P{^{1}H} NMR spectrum of 3.

Reaction of 1 with Thiophenol. Rh(I) complexes with phosphine ligands were reported to undergo oxidative addition of protic compounds such as HCl and HSPh to give Rh(III) hydride complexes. Reaction of 1 with HSPh also gives two isomeric Rh(III) hydride complexes depending on the reaction conditions. Addition of HSPh to a hexane solution immediately causes precipitation of a pale brown solid which can be separated from the reaction mixture by filtration. Further stirring of the reaction mixture without filtration of the initial product causes gradual dissolution of the pale brown solid accompanied by formation of yellow-green crystals. The two isolated products were characterized as *cis,mer*-RhH(SPh)$_2$(PMe$_3$)$_3$ (**4a**) (pale brown solid) and *trans,mer*-RhH(SPh)$_2$(PMe$_3$)$_3$ (**4b**) (yellow green crystals) on the basis of the NMR spectra and/or X-ray crystallography and are shown as follows: The ^{31}P{^{1}H} NMR spectrum of **4b**

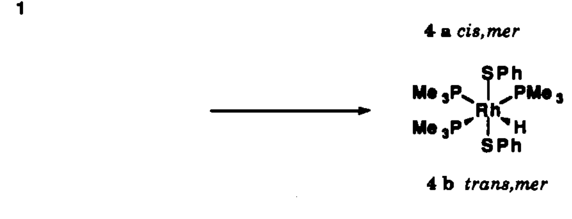

4 a *cis,mer*

4 b *trans,mer*

---

(35) Beach, D. L.; Garin, D. L.; Kaempfe, L. A.; Barnett, K. W. *J. Organomet. Chem.* **1977**, *142*, 211.

(36) (a) Dudley, C. W.; Read, G. *Tetrahedron Lett.* **1972**, 5273. (b) Dudley, C. W.; Read, G.; Walker, P. J. C. *J. Chem. Soc., Dalton Trans.* **1974**, 1926.

(37) Pregosin, P. S.; Kunz, W. *^{31}P and ^{13}C NMR of Transition Metal Phosphine Complexes*; Springer-Verlag: Heidelberg, Germany, 1979; pp 65–68.

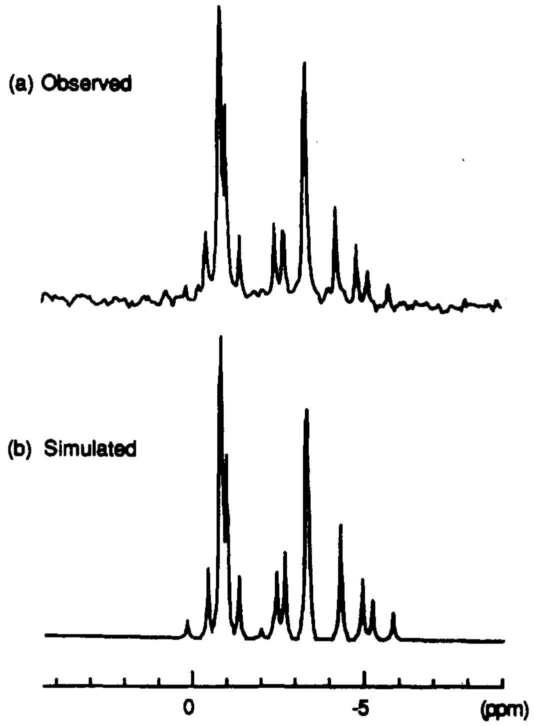

Figure 4. (a) Observed and (b) computer-simulated $^{31}P\{^1H\}$ NMR spectra of **3**.

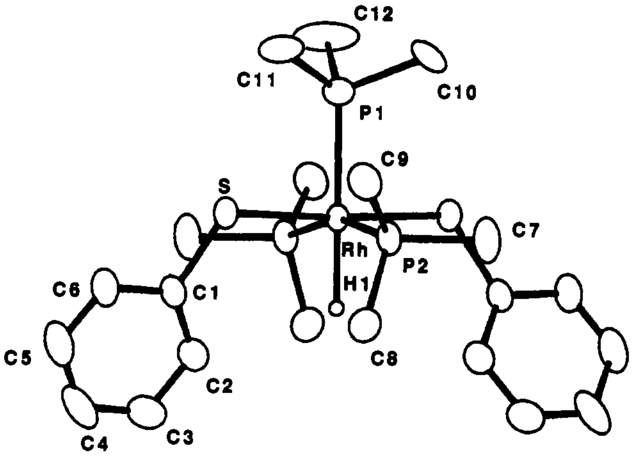

Figure 5. Molecular structure of *trans,mer*-RhH(SPh)$_2$(PMe$_3$)$_3$ (**4b**) showing ellipsoidal plotting at 30% level. The molecule has a crystallographic C_2 symmetric axis along the H1–Rh–P1 bonding arrangement. The carbon atoms of the PMe$_3$ ligand trans to the hydride ligand consequently show disorder of the positions. One of the two possible positions is shown. See text for details.

shows a triplet and a doublet (1:2 peak area ratio), indicating the meridional coordination of the PMe$_3$ ligands. The hydride signal in the ^{1}H NMR spectrum of **4b** shows a ^2J (PH) value (184 Hz) that is much larger than the other ^2J (PH) and ^1J(RhH) coupling constants (18 Hz and 11 Hz, respectively), indicating the trans mer structure having the hydride and a PMe$_3$ ligand at mutually trans positions. X-ray crystallography of **4b** shows more clearly the trans mer coordination as shown in Figure 5. Table III summarizes bond distances and angles. The NMR spectra of **4a** agree well with the cis mer structure.

Although oxidative addition of organic molecules to Wilkinson type Rh(I) complexes was reported in many cases, the stereochemistry was not well discussed. Previously Sacco and his coworkers have reported that oxidative addition of HCl to RhCl(PEt$_2$Ph)$_3$ gave two isomeric Rh(III) products depending on the reaction conditions.[38] They did not determine the structures of the complexes at that time, while the structure of the thermodynamically more stable isomer was later assigned as trans,mer coordinated on the basis of the ^{1}H NMR spectra.[39]

Table III. Selected Bond Distances and Angles of **4b**

	Distances (Å)		
Rh–S	2.384(1)	Rh–P1	2.394(2)
Rh–P2	2.330(1)	Rh–H1	1.69(7)
S–C1	1.761(4)	P1–C10	1.954(11)
P1–C11	1.962(11)	P1–C12	1.660(12)
P2–C7	1.814(5)	P2–C8	1.808(5)
P2–C9	1.818(5)		
	Angles (deg)		
S–Rh–S	176.77(6)	S–Rh–P1	88.39(3)
S–Rh–P2	85.44(4)	S–Rh–P2	95.07(4)
S–Rh–H1	91.61(3)	P1–Rh–P2	99.03(3)
P1–Rh–H1	180.0	P2–Rh–P2′	161.94(6)
P2–Rh–H1	80.97(3)	Rh–S–C1	116.3(1)

In order to elucidate the mechanism of the isomerization of **4a** to **4b**, reaction of labeled thiophenol with **4a** was examined. Reaction of DSPh (isotopic purity = 65%) with **4a** gives **4b** with deuterated hydrido ligand *trans,mer*-RhD(SPh)$_2$(PMe$_3$)$_3$ (**4b**-d_1) with isotopic purity of 55%. Although similar reaction of DSPh with **4b** also gives partially deuterated **4b**, the isotopic purity is much lower (18%). These results indicate that the cis to trans isomerization of the complex is accompanied by deuterium incorporation into the complex. This agrees with the isomerization mechanism that involves reductive elimination of PhSH from **4a** followed by immediate oxidative addition of PhSH to the Rh(SPh)(PMe$_3$)$_3$ to give **4b**.

Reaction of Complex 1 with Phenylacetylene. Complex **1** reacts with phenyl acetylene to give the oxidative addition product *trans,mer*-RhH(C$\equiv$CPh)(SPh)(PMe$_3$)$_3$ (**5**) as a white solid. NMR (^{1}H, $^{31}P\{^1H\}$, and $^{13}C\{^1H\}$) spectra of **5** agree with the structure. Signals of the PMe$_3$ hydrogens in the ^{1}H NMR and $^{31}P\{^1H\}$ NMR signals appear similarly to those of **4b**, indicating trans,mer-coordination of **5**. Formation of the cis, mer isomer was not observed in the reaction mixture. At this moment we cannot decide whether the oxidative addition of phenylacetylene proceeds through trans addition as is different from that of PhSH or through cis addition giving the intermediate *cis,mer*-RhH(C:CPh)(SPh)(PMe$_3$)$_3$ that undergoes rapid isomerization into **5** having the trans structure.

Concluding Remarks

Use of nonlabile PMe$_3$ in the preparation of rhodium thiolato complexes provided mononuclear Rh(I) complex **1** with a nonbridging thiolato ligand. The metal center of the complex shows high reactivity toward the oxidative addition of S–H and C–H bonds to give Rh(III) complexes with thiolato ligands. Since the thiolato ligand of **1** is also expected to show various reactivity, the complex is a promising starting material for various novel rhodium complexes.

Experimental Section

All the manipulations of the complexes were carried out under nitrogen or argon using Schlenk techniques.[40] [Rh(PMe$_3$)$_4$]Cl and RhCl(PMe$_3$)$_3$ were prepared according to the literature method.[33] NaSPh and NaSC$_6$H$_4$-*p*-OMe were prepared by reaction of the corresponding thiols with sodium ethoxide in ethanol and stored under nitrogen atmosphere. DSPh was prepared by reaction of concentrated DCl with NaSPh. The ^{1}H NMR spectrum shows the isotopic purity of 65%. IR spectra were recorded on a JASCO-IR810 spectrophotometer. NMR spectra (^{1}H, ^{13}C, and ^{31}P) were recorded on JEOL FX-100 and GX-500 spectrometers. Elemental analyses were carried out by a Yanagimoto Type MT-2 CHN autocorder and Yazawa halogen and sulfur analyzer. Rigaku AFC-5

---

(38) Sacco, A.; Ugo, R.; Moles, A. *J. Chem. Soc., (A)* **1966**, 1670.
(39) Henderson, R. A. *J. Chem. Soc., Dalton Trans.* **1985**, 2067.
(40) Yamamoto, A. *Organotransition Metal Chemistry. Fundamental Concepts and Applications*; John Wiley: New York, 1986.

Table IV. Crystallographic Data for Complexes **1**, **2**, and **4b**

complex	**1**	**2**	**4b**
chem formula	$C_{15}H_{32}P_3S_1Rh_1$	$C_{15}H_{32}O_2P_3S_1Rh_1$	$C_{21}H_{38}P_3S_2Rh_1$
fw	440.05	472.29	550.48
cryst system	orthorhombic	monoclinic	monoclinic
space group	*Pnma* (No. 62)	$P2_1$ (No. 4)	*I*2/*a* (No. 15)
a, Å	13.398(2)	12.197(2)	16.783(5)
b, Å	17.668(3)	9.307(2)	9.812(3)
c, Å	9.318(3)	9.427(3)	16.191(3)
β, deg		99.61(2)	93.88(2)
V, Å^3	2205.6	1055.1	2660.0
Z	4	2	4
μ, cm^{-1}	10.60	11.19	9.66
F(000)	912	456	572
ρ_{calcd}, g cm^{-3}	1.326	1.487	1.375
cryst size, mm	0.35 × 0.35 × 0.55	0.30 × 0.30 × 0.45	0.20 × 0.35 × 0.60
2θ range, deg	5.0–50.0	3.0–55.0	5.0–50.0
scan rate, deg min^{-1}	4	4	4
hkl	$0 \le h \le 20$	$-13 \le h \le 13$	$0 \le h \le 18$
	$-15 \le k \le 0$	$0 \le k \le 12$	$0 \le k \le 11$
	$0 \le l \le 11$	$0 \le l \le 12$	$-19 \le l \le 19$
no. of unique reflcns	1820	2470	2587
no. of used reflcns ($F_o \ge 3\sigma(F_o)$)	1351	2202	2015
$R(F_o)^a$	0.043	0.035	0.035
$R_w(F_o)^a$	0.046	0.032	0.050
weighting scheme	$[\{\sigma(F_0)\}^2]^{-1}$	$[\{\sigma(F_o)\}^2 + \{0.022(F_o)\}^2]^{-1}$	$[\{\sigma(F_o)\}^2]^{-1}$

[a] $R = \sum|F_o - F_c|/\sum|F_o|$; $R_w = [\sum w|F_o - F_c|^2/\sum w|F_o|^2]^{1/2}$.

and AFC-5R diffractometers were used for X-ray crystal structure determination using graphite-monochromated Mo Kα radiation (λ = 0.7107 Å). Structure calculations were carried out by using the program system CRYSTAN on a FACOM A-70 computer.

Preparation of Rh(SPh)(PMe$_3$)$_3$ (1). (a) From [Rh(PMe$_3$)$_4$]Cl. To a Schlenk flask containing [Rh(PMe$_3$)$_4$]Cl (390 mg, 0.88 mmol) and NaSPh (150 mg, 1.1 mmol) was added hexane (15 mL) by a syringe at room temperature. The resulting orange mixture was stirred at room temperature for 18 h to give a red reaction mixture containing a deposited white solid. Filtration of the solid followed by cooling the filtrate at –20 °C for 12 h gave an orange red solid (280 mg), which was filtered off. A total of 116 mg of the above solid was recrystallized from hexane to give Rh(SPh)(PMe$_3$)$_3$ (**1**) as red crystals (25 mg, 22%). ^{1}H NMR (100 MHz, in C_6D_6): δ 1.15 (bs, 27H, P(CH$_3$)$_3$), 8.3–6.9 (m, 5H, C_6H_5). ^{31}P{^{1}H} NMR (40 MHz in C_6D_6, ppm from external H_3PO_4): –13.51 (bs). Temperature-dependent ^{1}H and ^{31}P{^{1}H} NMR spectra (500 and 200 MHz, respectively) are shown in Figure 2.

(b) From RhCl(PMe$_3$)$_3$. A Schlenk flask containing RhCl(PMe$_3$)$_3$ (78 mg, 0.21 mmol) and NaSPh (36 mg, 0.27 mmol) was connected to a vacuum line. Hexane (7 mL) was transferred from a flask attached to the vacuum line to the Schlenk flask by cooling with liquid N_2. The reaction mixture was stirred for 24 h. After removal of the deposited NaCl by filtration the filtrate was set at room temperature. After several days red crystals of **1** formed (42 mg, 45%). Anal. Calcd for $C_{15}H_{32}P_3SRh$: C, 40.9; H, 7.3; S, 7.3. Found: C, 41.0; H, 7.6; S, 7.4.

Preparation of Rh(SPh)(O$_2$)(PMe$_3$)$_3$ (2) and Rh(SC$_6$H$_4$-*p*-OMe)(O$_2$)(PMe$_3$)$_3$ (3). To a Schlenk flask containing [Rh(PMe$_3$)$_4$]Cl (154 mg, 0.35 mmol) and NaSPh (62 mg, 0.47 mmol) was added hexane (15 mL) by a syringe. After stirring of the reaction mixture for 24 h, the resulting white solid was removed by filtration. Air introduction for 20 min to the filtrate causes formation of Rh(SPh)(O$_2$)(PMe$_3$)$_3$ (**2**) as orange crystals, which were filtered out, washed with hexane, and dried in vacuo (123 mg 75%). ^{1}H NMR (CD_2Cl_2): δ 1.29 (t by virtual coupling, 18H, P(CH$_3$)$_3$), 1.51 (d, 9H, P(CH$_3$)$_3$, *J* = 9 Hz), 7.5–6.7 (m, 5H, C_6H_5). ^{31}P{^{1}H} NMR (CD_2Cl_2, ppm from external H_3PO_4): 2.0 to –4.0 (m, simulated as A_2BX pattern with P_a = 0.1 (*J* = 36 and 130 Hz) and P_b = –1.4 (*J* = 36 and 139 Hz). Anal. Calcd for $C_{15}H_{32}O_2P_3SRh$: C, 38.1; H, 6.8; S, 6.8. Found: C, 37.9; H, 7.2; S, 6.9.

Introduction of air to **1** in the solid state also gave **2** in a quantitative yield.

Reaction of [Rh(PMe$_3$)$_4$]Cl (101 mg, 0.23 mmol) and NaSC$_6$H$_4$-*p*-OMe (45 mg, 0.28 mmol) followed by introduction of air into the reaction mixture gave Rh(SC$_6$H$_4$-*p*-OMe)(O$_2$)(PMe$_3$)$_3$ (**3**) in 73%. ^{1}H NMR (CD_2Cl_2): δ 1.29 (t by virtual coupling, 18H, P(CH$_3$)$_3$), 1.51 (d, 9H, P(CH$_3$)$_3$, *J* = 9 Hz), 3.69 (s, 3H, OCH$_3$), 7.5–6.5 (m, 4H, C_6H_4); ^{31}P{^{1}H} NMR (C_6D_6, ppm from external H_3PO_4), –0.5 to –6.0 (m, simulated as an A_2BX pattern with P_a = –2.0 ppm (*J* = 32 and 96 Hz), P_b = –3.3 ppm (*J* = 32 and 143 Hz). Anal. Calcd for $C_{16}H_{34}O_3P_3SRh$: C, 38.3; H, 6.8; S, 6.4. Found: C, 38.9; H, 7.3; S, 6.4.

Preparation of 4a and 4b. A hexane (5 mL) solution of HSPh (28 mg, 0.25 mmol) was added to the hexane (15 mL) solution containing complex **1** prepared from [Rh(PMe$_3$)$_4$]Cl (110 mg, 0.25 mmol) and NaSPh (44 mg, 0.33 mmol) in situ. A pale brown solid precipitated immediately was filtered off and dried in vacuo to give *cis,mer*-RhH(SPh)$_2$(PMe$_3$)$_3$ (**4a**) as a pale brown powdery solid (90 mg, 65% based on [Rh(PMe$_3$)$_4$]Cl). ^{1}H NMR (C_6D_6): δ –13.61 (ddd, 1H, RhH, *J* = 17, 17, and 17 Hz), 1.24 (t by virtual coupling, 18H, P(CH$_3$)$_3$), 0.95 (d, 9H, P(CH$_3$)$_3$, *J* = 7 Hz), 8.3–6.9 (m, 5H, C_6H_5). ^{31}P{^{1}H} NMR (C_6D_6, ppm from external H_3PO_4): –6.0 to –10.5 (m, simulated as an A_2BX pattern with P_a = –8.8 ppm (*J* = 55 and 90 Hz), P_b = –8.2 ppm (*J* = 55 and 110 Hz). IR (KBr): 2028 (s, ν(Rh–H)). Anal. Calcd for $C_{21}H_{38}P_3S_2Rh$: C, 45.8; H, 7.0; S, 11.6. Found: C, 46.1; H, 7.2; S, 13.5.

Stirring the above reaction mixture for 7 days caused disappearance of **4a** and formation of yellow crystals of *trans,mer*-RhH(SPh)$_2$(PMe$_3$)$_3$ (**4b**).

Complex **1** (120 mg, 0.23 mmol) was dissolved in toluene (5 mL) at room temperature. Stirring the reaction mixture at room temperature caused a change of the color of the mixture from orange to pale green. Addition of hexane (10 mL) followed by removal of the solvent (to ca. 2 mL) and further addition of hexane (5 mL) caused formation of yellow crystals of *trans,mer*-RhH(SPh)$_2$(PMe$_3$)$_3$ (**4b**) (100 mg, 79%). ^{1}H NMR (C_6D_6): δ –8.58 (ddd, 1H, RhH, *J* = 11, 18, and 184 Hz), 1.23 (t by virtual coupling, 18H, P(CH$_3$)$_3$), 1.03 (d, 9H, P(CH$_3$)$_3$, *J* = 7 Hz), 8.2–6.8 (m, 5H, C_6H_5). ^{31}P{^{1}H} NMR (C_6D_6, ppm from external H_3PO_4): –10.63 (dd, *J* = 96 and 27 Hz), –28.68 (dt, *J* = 82 and 27 Hz). IR (KBr): 2020 (m, ν(Rh–H)). Anal. Calcd for $C_{21}H_{38}P_3S_2Rh$: C, 45.8; H, 7.0; S, 11.6. Found: C, 46.0; H, 7.4; S, 11.1.

Reactions of DSPh with 4a and with 4b. To a toluene (5 mL) solution of **4a** (116 mg, 0.21 mmol) was added DSPh (108 mg, 0.97 mmol, 65% D) at room temperature. After stirring of the reaction mixture for 24 h at room temperature, the solvent was reduced to ca. 1 mL to give yellow crystals, which were filtered off and washed with hexane (74% as **4b**). The deuterium content of the hydride ligand of the obtained **4b** was determined as 55% by ^{2}H NMR using toluene-d_8 as the internal standard.

Similar reaction of **4b** with DSPh gave **4b** deuterated in 18%.

Preparation of 5. A hexane (5 mL) solution of phenylacetylene (35 mg, 0.34 mmol) was added to a hexane (15 mL) solution containing complex **1** prepared in situ from [Rh(PMe$_3$)$_4$]Cl (150 mg, 0.34 mmol) and NaSPh (53 mg, 0.40 mmol). Stirring for 3 min caused precipitation of a white solid of *trans,mer*-RhH(C≡CPh)(SPh)(PMe$_3$)$_3$ (**5**), which was filtered off, washed with hexane, and dried *in vacuo* (133 mg, 72% based on [Rh(PMe$_3$)$_4$]Cl). ^{1}H NMR (C_6D_6): δ –8.69 (ddd, 1H, RhH, *J* = 16, 16, and 191 Hz), 1.32 (bs, 18H, P(CH$_3$)$_3$), 1.09 (d, 9H, P(CH$_3$)$_3$, *J* = 7 Hz). ^{31}P{^{1}H} NMR (C_6D_6, ppm from external H_3PO_4): –9.45 (dd, *J* = 94 and 27 Hz), –27.29 (dt, *J* = 78 and 27 Hz). ^{13}C{^{1}H} NMR (C_6D_6): 105.04 (m, C–Ph), 106.04 (ddt, Rh–C, *J* = 15, 18 and 42 Hz), 140.82 (dd, S–C, *J* = 10 and 9 Hz). Anal. Calcd for $C_{23}H_{38}P_3SRh$: C, 50.9; H, 7.1; S, 5.9. Found: C, 50.0; H, 6.9; S, 7.0.

Table V. Atomic Coordinates and Equivalent Isotropic Temperature Factors of **1**

atom	*x*	*y*	*z*	B_{eq}, Å^2
Rh	0.11935(5)	0.2500	0.20613(7)	3.18
S	−0.0002(1)	0.2500	0.0778(3)	4.0
P1	0.1023(1)	0.0810(1)	0.2259(2)	4.6
P2	0.2425(1)	0.2500	0.2579(3)	4.6
C1	0.0245(6)	0.2500	−0.1038(9)	4.0
C2	−0.0314(6)	0.2500	−0.2078(11)	5.0
C3	−0.0130(10)	0.2500	−0.3534(13)	7.4
C4	0.0588(1)	0.2500	−0.3975(14)	8.9
C5	0.1162(9)	0.2500	−0.2935(15)	10.1
C6	0.0982(7)	0.2500	−0.1492(12)	6.7
C7	0.1582(6)	0.0055(7)	0.3536(12)	10.0
C8	0.1086(5)	0.0093(6)	0.0627(10)	7.9
C9	0.0095(5)	0.0496(5)	0.2939(9)	6.2
C10	0.2786(7)	0.2500	0.4373(13)	10.8
C11	0.2978(5)	0.1484(8)	0.1789(13)	10.6

Table VI. Atomic Coordinates and Equivalent Isotropic Temperature Factors of **2**

atom	*x*	*y*	*z*	B_{eq}, Å^2
Rh	0.20803(2)	0.50000	0.80567(3)	2.09
S	0.3691(1)	0.3910(2)	0.7373(2)	2.99
P1	0.1381(1)	0.2941(2)	0.8999(2)	3.07
P2	0.2338(1)	0.7006(2)	0.6664(2)	3.14
P3	0.3227(1)	0.5708(2)	1.0120(2)	2.91
O1	0.0653(3)	0.4984(7)	0.6576(4)	3.38
O2	0.0481(3)	0.5605(4)	0.7938(4)	3.72
C1	0.3337(5)	0.2736(6)	0.5897(6)	2.7
C2	0.2258(5)	0.2482(7)	0.5192(6)	3.3
C3	0.2049(5)	0.1512(8)	0.4075(7)	4.2
C4	0.2900(6)	0.0792(7)	0.3633(7)	4.5
C5	0.3977(6)	0.1024(8)	0.4295(7)	4.4
C6	0.4202(5)	0.1987(7)	0.5421(7)	3.7
C7	0.0668(5)	0.3258(8)	1.0494(7)	5.2
C8	0.2306(6)	0.1422(7)	0.9581(8)	5.2
C9	0.0284(5)	0.2127(7)	0.7738(7)	4.5
C10	0.1196(6)	0.8260(7)	0.6515(7)	4.5
C11	0.2371(6)	0.6482(8)	0.4839(6)	4.4
C12	0.3538(6)	0.8172(8)	0.6992(8)	5.5
C13	0.2776(7)	0.7356(8)	1.0835(7)	5.3
C14	0.4668(5)	0.6047(8)	1.0016(7)	4.8
C15	0.3437(6)	0.4577(7)	1.1718(7)	5.1

Similar reaction of phenylacetylene with a reaction mixture of $RhCl(PMe_3)_4$ with $NaSC_6H_4$-*p*-OMe gave *trans,mer*-RhH-(C≡CPh)(SC_6H_4-*p*-OMe)$(PMe_3)_3$ (**6**) in 84% yield. ^{1}H NMR (C_6D_6): δ −8.72 (ddd, 1H, RhH, J = 16, 17, and 192 Hz), 1.34 (bs, 18H, $P(CH_3)_3$), 1.12 (d, 9H, $P(CH_3)_3$, J = 7 Hz), 3.39 (s, 3H, OCH_3). $^{31}P\{^1H\}$ (C_6D_6, ppm from external H_3PO_4): −9.40 (dd, J = 94 and 27 Hz), −27.19 (dt, J = 78 and 27 Hz). Anal. Calcd for $C_{24}H_{40}OP_3SRh$: C, 50.4; H, 7.0; S, 5.6. Found: C, 49.9; H, 7.4; S, 5.6.

X-ray Structural Characterization. Table IV summarizes crystal data of the complexes. Tables V–VII show atomic coordinates and equivalent isotropic temperature factors of **1**, **2**, and **4b**, respectively.

Complex 1. Orange blocks of **1** were grown in hexane at room temperature. Cell constants were determined and refined on the basis of setting angles of 25 reflections with 2θ = 25–35°. Systematic absences of the intensity data agreed with the space groups *Pnma* (No. 62) and with $Pna2_1$ (No. 33). Structure calculations based on the former space group gave the molecular structure having a crystallographic mirror plane including Rh, S, P2, C1–C6, and C10 atoms and converged well to give final convergence R = 0.043 and R_w = 0.046, while structure calculation based on the latter space group did not converge well. The hydrogen atoms located at idealized positions were included in the structure calculation without refinement of their parameters.

Table VII. Atomic Coordinates and Equivalent Isotropic Temperature Factors of **4b**

atom	*x*	*y*	*z*	B_{eq}, Å^2
Rh	0.25	0.57760(5)	0.00	2.92
S	0.35637(6)	0.57076(11)	0.10527(7)	3.94
P1	0.25	0.3336(2)	0.0	6.0
P2	0.16773(6)	0.61487(12)	0.10811(7)	3.74
C1	0.4119(2)	0.7218(5)	0.1211(2)	3.7
C2	0.3971(3)	0.8420(5)	0.0804(3)	4.8
C3	0.4472(4)	0.9546(6)	0.0952(4)	6.2
C4	0.5113(4)	0.9457(7)	0.1517(4)	7.2
C5	0.5260(3)	0.8249(7)	0.1940(4)	6.3
C6	0.4777(3)	0.7152(6)	0.1792(3)	4.7
C7	0.0604(5)	0.6168(6)	0.0851(3)	5.6
C8	0.1849(3)	0.7816(5)	0.1534(3)	4.9
C9	0.1774(3)	0.5076(6)	0.1998(3)	5.2
C10	0.1433(7)	0.2636(12)	0.0165(10)	7.3
C11	0.2949(10)	0.2526(11)	0.1038(9)	7.7
C12	0.2803(13)	0.2278(13)	−0.0715(11)	10
H1	0.25	0.749(7)	0.0	7[a]

[a] An isotropic thermal factor was applied.

Complex 2. Yellow orange blocks of **2** were grown in dichloromethane at −20 °C. Cell constants were determined and refined on the basis of setting angles of 25 reflections with 2θ = 18–22°. Systematic absences of the intensity data agreed with the space groups $P2_1$ (No. 4) and with $P2_1/m$ (No. 11). The former space group was chosen since the calculation based on the latter did not give any reasonable crystal structure. Structure calculations were carried out by applying anisotropic thermal factors for the non-hydrogen atoms and isotropic thermal factors for the hydrogen atoms, which were located at idealized positions, to give final convergence R = 0.0347 and R_w = 0.0318. Although the complex **2** does not have a chiral center, the molecular structure in the crystals has two possible chiral conformations due to the chiral space group. Calculations based on the structure with chirality opposite to that of the structure in Figure 3 gave final convergence of $R = 0.035_7$ and $R_w = 0.032_7$, which are worse than the convergence in the calculations based on the right structure. Agreement of the distances of the chemically equivalent Rh–P1 and Rh–P2 bonds is much better in the right hand than in the wrong hand.

Complex 4b. Yellow prisms of **4b** were grown in hexane at −20 °C. Cell constants were determined and refined on the basis of setting angles of 25 reflections with 2θ = 25–35°. Systematic absence of the intensity data agreed with the space group *I*2/*a* (No. 15) and with *Ia* (No. 7). Structure calculation based on the former space group gave the molecular structure having a crystallographic 2-fold axis along the linear H–Rh–P3 bonding arrangement and converged well to give final convergence R = 0.035 and R_w = 0.050, while the calculation based on the latter space group did not converge well. The crystallographic 2-fold symmetry requires that the unique PMe_3 group be disordered. The hydrogen atom bonded to the Rh atom was reasonably observed on the 2-fold axis in the difference map, and the position was refined isotropically. The hydrogen atoms attached to the disordered carbon atoms were not included in the structure calculation. All the other hydrogen atoms were located at idealized positions. These hydrogen atoms were included in the structure calculation without refinement of the parameters.

Acknowledgment. This work was financially supported by Grants-in-Aid for Scientific Research from the Ministry of Education, Science, and Culture (03855182 and 04805084). The authors are grateful to Drs. Masako Tanaka and Yoshiyuki Nakamura in our laboratory for their help in crystallography and NMR measurements, respectively.

Supplementary Material Available: Figures showing the molecular structures including hydrogen atoms of **1**, **2**, and **4b** with atomic numbering schemes and tables listing anisotropic thermal factors, fractional coordinates of the hydrogen atoms, and all the bond distances and angles (19 pages). Ordering information is given on any current masthead page.